Spatial distribution of CD34 protein in primordial odontogenic tumour, ameloblastic fibroma and the tooth germ.

Pereira Prado, Vanesa; Landini, Gabriel; Taylor, Adalberto Mosqueda; Vargas, Pablo; Bologna Molina, Ronell

DOI:
10.1111/jop.13370

Spatial distribution of CD34 protein in primordial odontogenic tumour, ameloblastic fibroma and the tooth germ.

Vanesa Pereira Prado[1], Gabriel Landini[2], Adalberto Mosqueda Taylor[3], Pablo Vargas[4], Ronell Bologna Molina[1].

1 Molecular Pathology Area, Facultad de Odontología, Universidad de la República, Montevideo, Uruguay. ORCID

Vanesa Pereira Prado

- ORCID: 0000-0001-7747-6718.
- E-mail: vanesapereira91@hotmail.com

Ronell Bologna Molina

- ORCID: 0000-0001-9755-4779.
- E-mail: ronellbologna@hotmail.com

2 School of Dentistry, College of Medical and Dental Sciences, University of Birmingham, Edgbaston, Birmingham, United Kingdom. ORCID: 0000-0002-9689-0989. E-mail: G.Landini@bham.ac.uk

3 Health Care Department, Universidad Autónoma Metropolitana Xochimilco, Mexico City, Mexico. ORCID: 0000-0001-8956-6016. E-mail: mosqueda@correo.xoc.uam.mx

4 Department of Oral Diagnosis, Piracicaba Dental School, University of Campinas, Piracicaba, Brazil. ORCID: 0000-0003-1840-4911. E-mail: pavargas@unicamp.br

Dra. PEREIRA reports grants from CSIC and from SANTANDER UDELAR, during the conduct of the study. The rest of the authors declare that they do not have a conflict of interest.

Ethical Committee approval was received for the present study: Universidad de la República, Facultad de Odontología, Uruguay (21/11/19, Exp. No. 091900-000319-19).

Abstract

Background: Primordial odontogenic tumour is a benign mixed neoplasm of recent description, which has histological similarities with other odontogenic tumours such as the ameloblastic fibroma. In this paper, we investigate the architecture of the sub-epithelial layer of mesenchymal cells expressing the marker CD34 in primordial odontogenic tumour.

Objective: Analyse the spatial patterns of CD34 expression in primordial odontogenic tumour and compare them with those in ameloblastic fibroma and the normal tooth germ by means of objective imaging approaches, in order to better characterise these lesions.

Methods: Two cases of primordial odontogenic tumour, four cases of ameloblastic fibroma and two cases of tooth germ in cap and bell stages were used for morphological, structural and immunohistochemical analyses.

Results: CD34 expression was found in vascular endothelium of primordial odontogenic tumour, ameloblastic fibroma and tooth germ. In addition, a characteristic sub-epithelial expression was observed only in primordial odontogenic tumour, corresponding to 84-86% of the sample boundaries. Moreover, the zone expressing CD34 corresponded with a higher cellularity, which was absent in ameloblastic fibroma and tooth germ.

Conclusion: Image analysis of the primordial odontogenic tumour architecture revealed characteristics absent in other odontogenic tumours and tooth germs.

This study provides additional information to support the idea that this neoplasm is a distinct entity from early stage AF or developing odontoma.

Key words: primordial odontogenic tumour, CD34, tooth germ, ameloblastic fibroma, odontogenesis.

Introduction

Primordial Odontogenic Tumour (POT) is a rare benign odontogenic neoplasm firstly described by Mosqueda Taylor et al. in 2014 (1). To date 22 cases have been reported worldwide (2-5). Histologically, POT is a mixed tumour, composed of dental papilla-like tissue covered by a cuboidal to columnar epithelium resembling the inner enamel epithelium of the enamel organ, which often invaginates into the underlying connective tissue, but does not induce dental hard tissue formation. The tumour is partly surrounded by a delicate fibrous capsule (1). Our group studied the immunoexpression of twenty-three different antigens in POT, which confirm its odontogenic origin from the primary stages of tooth development (cap-bell stages), and the presence of both epithelial and mesenchymal activity, with differential expression of certain markers in particular zones of both tissue components (6). This suggested that POT might arise during the early stages of tooth development, from the mesenchyme of an abortive tooth germ (TG) that fails to differentiate and consequently is not able to induce the formation of hard tissues. Some authors suggested POT to be an intermediate stage in the development of an odontoma (7); however, our group defined a series of criteria explaining their differences (8):

- POT is associated with a non-erupted tooth in an apparent pericoronal location.
- POT has absence of mineralized dental tissue and odontoblastic differentiation.
- POT presents increased cellularity at the interface between the epithelium surrounding the lesion and the underlying mesenchymal tissue.

The definitive diagnosis of odontogenic tumours is histopathological and because other mixed odontogenic neoplasms share some histological similarities with POT, such as ameloblastic fibroma (AF) and immature odontoma, it seems important to identify objective histomorphological characteristics and criteria that facilitate understanding their pathogenesis and facilitate diagnostic and prognostic decisions.

Our group previously reported CD34 expression in the mesenchymal component of POT in two locations: cells located close to the odontogenic epithelium (suggesting the presence of embryonic fibroblasts) and in the endothelium of blood vessels (6, 9). To our knowledge, that finding has not been described in other odontogenic tumours and appears to be a differential feature of POT. CD34 is a transmembrane protein highly expressed in immature haematopoietic stem cells, endothelium of blood capillaries, embryonic fibroblasts and a multitude of other non-haematopoietic cell types, progressively decreasing in expression with stages of cell maturation (10). However, the significance of this morphological feature has not been systematically studied in POT. The aim of the present study is therefore to analyse the spatial patterns of CD34 expression in POT and compare these with those in AF and the normal

TG by means of objective imaging approaches, in order to better characterise these lesions.

Materials and methods

Two cases of POT were retrieved from Health Care Department, Universidad Autónoma Metropolitana Xochimilco, Mexico, four cases of AF and two cases of TG in cap and bell stages from the Department of Oral Diagnosis, Piracicaba Dental School, University of Campinas, Piracicaba, Brazil, were included in the present study. Ethical Committee approval was received for the present study: Universidad de la República, Facultad de Odontología, Uruguay (21/11/19, Exp. No. 091900-000319-19).

Immunohistochemistry

Three-micrometre sections of formalin fixed tissues embedded in paraffin blocks were set on glass slides previously treated with poly-lysine. Sections were then deparaffinized, rehydrated and antigen retrieval was performed through treatment with 0.1 M sodium citrate (pH 6.2) and Tween 20 in a microwave oven for 7 minutes to unmask the epitopes. Endogenous peroxidases were blocked with 0.9% hydrogen peroxide. Primary antibody for CD34 (Biocare/QBEnd10, 1:50 dilution) was incubated for 45 min at room temperature. Afterwards, the slides were incubated with a biotinylated anti-mouse/anti-rabbit antibody and the streptavidin/peroxidase complex for 30 min each (LSAB+-labelled streptavidin-biotin, Dako) and the reaction was visualised with 3, 3’-diaminobenzidine-H2O (Dako). Finally, the sections were counterstained with Mayer’s haematoxylin solution. Blood vessels within the mesenchymal tissue were considered as internal positive control. For the negative control, the

primary antibody was replaced with PBS. Results were visually assessed using an optical microscope (Eclipse Ci-L, Nikon, Japan) with a 40X objective.

Alcian blue + PAS stain

Alcian blue + PAS technique was also performed in POT cases to disclose any compositional tissue changes in the sub-epithelial regions. Deparaffinized and rehydrated slides were immersed in acetic acid solution 3% for 5 min. Afterwards the slides were stained with alcian blue 0.5% pH solution for 30 min at room temperature, periodic acid 0.5% for 10 min and Schiff reactive for 20 min. Finally, the sections were dehydrated in graded ethanol.

Digitization

A Motic EasyScan© scanner was used for slide digitization with a x40 objective in standard mode. Pathomation's PMA.start software (11) was used for visualisation and capture of regions of interest. Every area with presence of odontogenic epithelium was considered a region of interest in the three entities studied. For POT and TG specimens, the upper border of the image frame was used as reference to align the epithelial component so that all images could be comparably aligned. RGB images (representing regions of interest of which corresponded to a field of view of 315 x 638μm) were saved in TIFF format for further analysis.

CD34 analysis as a function of depth

POT boundaries were analysed in CD34 stained samples in order to estimate the proportion (%) of the tumour boundary length where the sub-epithelial zone was positive for this marker. To accomplish this, the ImageJ (12) freehand line

tool was used and length measurements were determined in both POT tumours.

Images of CD34 stained samples of POT and TG were further analysed using an ImageJ macro that computed the presence of positive CD34 immunostain from the image upper border (that corresponds to the tumour outer boundary epithelium) to the bottom border (which corresponds to a maximum depth of 638μm), i.e. to provide a measure of the presence of CD34 staining in function of tumour depth. The regions containing the IHC product were computed using stain unmixing (colour deconvolution) (13), then thresholded using Otsu's method (12). Immunohistochemistry uses a chromogenic precipitation for visualisation of the immunoreactivity, which is difficult to control, and therefore the stained product is non-stoichiometric. Therefore, a binary (presence/absence) approach was used to detect the spatial distribution of staining across each sample rather than attempting to quantify staining intensities. The distance from the pixels in these regions to the border of the tissue were determined using the 'Euclidean distance transform' in ImageJ and a histogram of distances computed for the ensemble of POT samples.

The approach, however, needs to be modified when applied to AF samples because of a difference in geometry and topology of the epithelium in this neoplasm when compared to POT and TG: while POT and TG contain an outer epithelial layer, AF consists of multiple epithelial islands and the distance from these to other the mesenchymal components of interest is not a function of the depth from the outer tissue boundary and so the segmentation requires a different approach. To this end, Fiji's Labkit segmentation plugin (14) was used first to determine the epithelial component by 'training' a classifier to recognise

image pixels belonging to three tissue classes of interest (which were annotated interactively by the operator): i.e. mesenchymal tissue, CD34+ regions and epithelial islands. The result of the training is a three-phase segmented image and the classifier can be used to segment unseen images. Then, the Euclidean distance transform was applied to the pixels labelled as non-epithelial regions to compute their distance to the nearest segmented epithelium region. Subsequently, the CD34 labelled regions were queried to retrieve the value of the previously computed distance transform to the nearest epithelial component. The distance from the epithelial islands to the CD34 positive regions was also determined the 'Euclidean distance transform' as described earlier. These procedures were repeated in 99 POT images, 62 AF images and 8 TG images.

In addition, the epithelial thickness in POT and TG was measured interactively with using ImageJ's straight line tool to be able to compensate for the difference in position of the epithelial-connective tissue interface (ECTI) when comparing to AF images (discussed below).

Results

Alcian blue + PAS stain

The alcian blue + PAS staining on the POT sections revealed sky-blue regions showing the presence of mucopolysaccharides notably in the sub-epithelial regions. This suggested a functionally distinct zone, which also coincided with a high cellular density when compared with the deeper parts of the neoplasm mesenchymal component (Fig.1).

Immunohistochemistry

CD34 expression was evident in the vascular endothelium of POT, AF and TG (Fig.2). In addition, positive expression was also observed in the sub-epithelial region of POT cases, approximately along 84-86% of the tissue boundaries and which coincided with the zone of increased cellularity and more intense alcian-blue staining mentioned earlier. Interestingly, in some locations where CD34 expression was absent, the sub-epithelial cellularity condensation also decreased.

CD34 analysis as a function of depth

The POT images of sections stained with CD34 antibodies showed a pattern of increasing cellularity when positive in the sub-epithelial area (Fig.3 A-C). Moreover, negative CD34 sub-epithelial expression correlated with a reduction of nuclear density (Fig.3 D-E).

CD34 positivity in AF was detected in the endothelium of blood vessels (Fig.4). These vessels could be seen near odontogenic epithelium islands, unlike in POT (Fig.6, black plot) where there is a vessel-free zone below the odontogenic epithelium. Figure 6 shows a scan plot of the probability of stained CD34 regions in AF, TG and POT, revealing a peak that progressively decreases in AF and POT cases, without discrimination to which structure CD34 positivity corresponds. In some cases of AF, there were only few small calibre vessels close to the epithelium.

The contribution of CD34 positive expression in TG seems to be exclusively due to the presence of blood vessel endothelium and it was similar to that of POT

areas where no sub-epithelial CD34 expression was found (Fig.5-6, black and blue plot).

The average POT epithelium thickness (27μm ± 19) and that of the TG (33μm ± 6) were used to offset the plots in Figure 6, so the ECTI position was comparable across the different samples.

In Fig. 6, the red plot (POT) reaches a maximum value at of 31μm (after smoothing the plot with a running average of 15 data points, not shown) which corresponds with the CD34 sub-epithelial expression; from then on, CD34 expression is due to the presence of vessels which progressively decrease towards the deeper connective. The black and blue plots show a relatively constant presence of CD34 vessels.

The AF data shows a different distribution of CD34 staining when compared with POT and TG, with a broad peak revealing positive regions peaking at about 96μm from the epithelial islands (after smoothing the plot with a running average of 15 data points, not shown). In addition, some samples of POT and AF featured a zone of hyalinization next to the epithelium.

Discussion

This systematic study of the architecture of POT, AF and TG based on the spatial distribution of the CD34 immunomarker suggests the presence of a distinct sub-epithelial area in regions of POT which are not from the vascular endothelium.

Our group previously noted this mesenchymal band of CD34 positive cells in POT beneath epithelial layers, suggesting these may represent embryonic fibroblasts (6, 7, 9). CD34 expression was observed in two distinct

compartments, namely the endothelium of blood vessels and in the mesenchymal cells adjacent to the epithelium. However, lack of CD34 expression in the sub-epithelial zone was also occasionally seen in some parts of the tumours (14-17%) which correlates also with less mesenchymal cell condensation. This could be interpreted as different stages of differentiation or early odontogenic induction, which might play an important role in tumorigenesis and appears to be a unique feature for this odontogenic tumour. Comparing this feature with that found in TG further suggests that the POT sub-epithelial nuclear condensation might be akin to the dental papilla condensation area observed in the stages preceding odontoblastic differentiation during odontogenesis. According to case reports of POT in the literature, several studies demonstrated CD34 positivity, while in nine cases no immunohistochemical analysis was mentioned (2-5).

Comparing POT CD34 expression in histopathologically similar tissues and with a similar histogenesis (AF and TG) showed some interesting differences: only POT appears to feature the CD34 positive sub-epithelial zone while AF and TG were negative in that location.

AF positive expression of CD34 was only seen in relation to endothelium of vessels; some of those vessels were observed in the proximity of epithelial islands. However, in POT no vessels seem to be present in the zone adjacent to the epithelium, regardless of the presence of the CD34+ zone. This comparison could be done since AF presented dental epithelium in a similar architecture with POT, although comparing POT with partial biopsies of AF may be challenging.

Expression of CD34 in the stroma of odontogenic lesions has been used for the assessment of microvascular density, in an attempt to elucidate the biological behaviour of these lesions (15). In this context, Chacham et al. (15) reported the presence of CD34 positive dendritic cells adjacent to the lining epithelium of recurrent odontogenic keratocysts, suggesting it could be a potential feature to differentiate from other, more mature cell types, such as myofibroblastic, adipogenic, osteoblastic and chondroblastic cells. Embryonic fibroblasts are often prominent in the reactive stroma associated with cancerous tissue and it has been hypothesised that they could be responsible for triggering effects on surrounding epithelial cells such as epithelial-mesenchymal transition, cell proliferation, angiogenesis, invasion and metastasis (16).

In this study, immunohistochemical expression of CD34 in TG tissue was observed (as in AF) limited to the dental papilla endothelium but was negative in cells near the epithelium at both cap and bell stages. While the tooth germ tissue is known to be rich in mesenchymal stem cells, according to Aydin et al., those cells express a variety of mesenchymal stem cell markers including CD146, CD106, CD90, CD29 and CD13, but interestingly they do not express haematopoietic stem cell markers such as CD34 (17). In a previous study, our group reported the presence of CD90 and CD105 in POT only limited to vascular endothelium (6). Therefore, in our study, CD34 sub-epithelial expression could represent a cell type different from the normal differentiation odontogenic process.

Moreover, alcian blue + PAS staining on POT revealed the presence of mucopolysaccharides in the sub-epithelial area. This finding differs from TG, were acid radicals seem to be present in the stellar reticulum, basal membrane

and deeper areas of mesenchymal dental papilla, decreasing while progressing in odontogenesis (18).

Notwithstanding that the POT histological features point to an origin from a primordial TG, the results reported here support the idea that POT is a distinct odontogenic neoplasm, morphologically different from the other established categories and furthermore, not a developing odontoma or an early stage AF as it has been proposed before (6, 9).

Histopathological image analysis through quantitative techniques provides novel approaches to structural analyses that can facilitate understanding tumor pathogenesis and facilitate diagnostic and prognostic decisions. Leaving aside the clinical considerations that can contribute to the diagnosis of these entities, it seems important to remark that POT does not induce odontoblastic differentiation or production of dentine proteins as observed in other odontogenic tumours such as odontoma. Furthermore, the absence of dense cellularity in the sub-epithelial regions of AF and TG emphasises architectural differences with POT. The CD34 expression pattern in the three tissues investigated suggests the presence of an immature cell type that could potentially induce epithelial-mesenchymal transition, proliferation and angiogenesis.

One limitation of the present study is the number of cases and images analysed due to the rarity of POT, but further studies based on the principles described may contribute to confirming the findings reported. The analysis of additional immunomarkers could also help to elucidate further details of the relation between architecture and behaviour of POT.

Conclusion

Image analysis of the POT architecture revealed characteristics not observed in other odontogenic tumours and TG. This study provides additional information to support the idea that this neoplasm is a distinct entity from early stage AF or developing odontoma.

References

1) Mosqueda-Taylor A, Pires FR, Aguirre-Urízar JM, Carlos-Bregni R, de la Piedra-Garza JM, Martínez-Conde R, Martínez-Mata G, Carreño-Álvarez SJ, da Silveira HM, de Barros Dias BS, de Almeida OP. Primordial odontogenic tumour: clinicopathological analysis of six cases of a previously undescribed entity. Histopathology. 2014 Nov; 65(5):606-12. doi: 10.1111/his.12451. Epub 2014 Sep 2. PMID: 24807692.

2) Delgado-Azañero WA, de Almeida OP, Pereira AAC, de Oliveira CE, Dias MA, Florez-Valderrama G, de Lima Morais TM, Mariz BALA, Mosqueda-Taylor A. Primordial odontogenic tumor: report of 2 new cases. Oral Surg Oral Med Oral Pathol Oral Radiol. 2021 Aug;132(2):e69-e77. doi: 10.1016/j.oooo.2020.08.004. Epub 2020 Aug 8. PMID: 32981867.

3) Kayamori K, Tsuchiya M, Michi Y, Kuribayashi A, Mikami T, Sakamoto K, Yoda T, Ikeda T. Primordial odontogenic tumor occurred in the maxilla with unique calcifications and its crucial points for differential diagnosis. Pathol Int. 2021 Jan;71(1):80-87. doi: 10.1111/pin.13036. Epub 2020 Oct 20. PMID: 33079412.

4) Zeng M, Chen X, Guo X, Yang S. Report of a classic primordial odontogenic tumour and an unusual mixed odontogenic tumour with features of

primordial odontogenic tumour: diagnostic implications. Pathology. 2020 Aug;52(5):596-599. doi: 10.1016/j.pathol.2020.04.007. Epub 2020 Jun 24. PMID: 32593436.

5) Naina S, Narwal A, Devi A, Kamboj M, Pandiar D. Primordial Odontogenic Tumor of Anterior Maxilla in a Young Male: A Case Report and an Updated Review of Literature. Pediatr Dev Pathol. 2021 Jan-Feb;24(1):73-79. doi: 10.1177/1093526620972589. Epub 2021 Jan 12. PMID: 33433252.

6) Bologna-Molina R, Mikami T, Pereira-Prado V, Pires FR, Carlos-Bregni R, Mosqueda-Taylor A. Primordial odontogenic tumor: An immunohistochemical profile. Med Oral Patol Oral Cir Bucal. 2017 May 1;22(3):e314-e323. doi: 10.4317/medoral.21859. PMID: 28390134; PMCID: PMC5432080.

7) Ide F, Kikuchi K, Kusama K, Muramatsu T. Primordial odontogenic tumour: is it truly novel? Histopathology. 2015 Mar;66(4):603-4. doi: 10.1111/his.12595. Epub 2014 Dec 23. PMID: 25358820.

8) Bologna-Molina R, Mosqueda-Taylor A. Primordial odontogenic tumour or developing odontoma? Histopathology. 2020 Feb;76(3):489-490. doi: 10.1111/his.13999. Epub 2019 Dec 11. PMID: 31545527.

9) Mikami T, Ohashi Y, Bologna-Molina R, Mosqueda-Taylor A, Fujiwara N, Tsunoda N, Yamada H, Takeda Y. Primordial Odontogenic Tumor: A case report with histopathological analyses. Pathol Int. 2017 Dec;67(12):638-643. doi: 10.1111/pin.12601. Epub 2017 Nov 1. PMID: 29090496.

10) Nishio H, Tada J, Hashiyama M, Hirn J, Ingles-Esteve J, Suda T. MC7. CD34 workshop panel report. In: Kishimoto T, Kikutani H, von dem Borne AEG, Goyert SM, Mason DY, Miyasaka M, et al. Leucocyte typing VI. White cell differentiation antigens. Proceedings of the 6th International Workshop

and Conference; 1996 Nov 10-14; Kobe, Japan. New York, London: Garland Publishing Inc.; 1997. p. 974-76.

11) Pathomation, Antwerp, Belgium. https://www.pathomation.com/

12) Rasband WS, ImageJ, U. S. National Institutes of Health, Bethesda, Maryland, USA, https://imagej.nih.gov/ij/, 1997-2022.

13) Landini G, Martinelli G, Piccinini F. Colour deconvolution: stain unmixing in histological imaging. Bioinformatics 2021, 37 (10), 1485-1487.

14) Arzt M, Deschamps J, Schmied C, Pietzsch T, Schmidt D, Tomancak P, Jug F. LABKIT: Labeling and Segmentation Toolkit for Big Image Data. Frontiers in Computer Science 2022. doi:10.3389/fcomp.2022.777728

15) Chacham M, Almoznino G, Zlotogorski-Hurvitz A, et al. Expression of stem cell markers in stroma of odontogenic cysts and tumors. J Oral Pathol Med. 2020;00:1–10. https://doi.org/10.1111/jop.13102.

16) Hanahan D and Weinberg RA. Hallmarks of cancer: the next generation. Cell 2011; 144: 646-674.

17) Aydin S, Şahin F. Stem Cells Derived from Dental Tissues. Adv Exp Med Biol. 2019;1144:123-132. doi: 10.1007/5584_2018_333. PMID: 30635857.

18) Quintarelli G, Dellovo M.C. Mucopolysaccharide histochemistry of rat tooth germs. Histochemie, 1963, 3(3), 195–207. doi:10.1007/bf00736437.

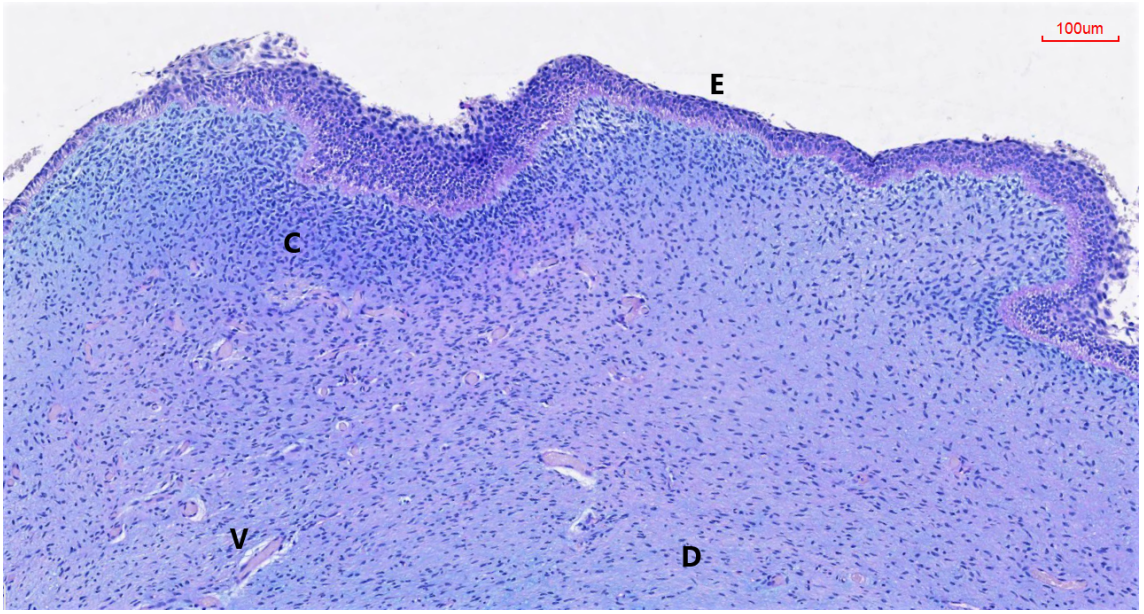

Fig. 1. Alcian blue + PAS stained POT. E: epithelium, C: condensed mesenchymal zone, V: vessels, D: deep mesenchymal zone. The sky-blue staining in the sub-epithelial region indicated the presence of mucopolysaccharides, which appear to be less obvious deeper in the tumour mesenchymal component.

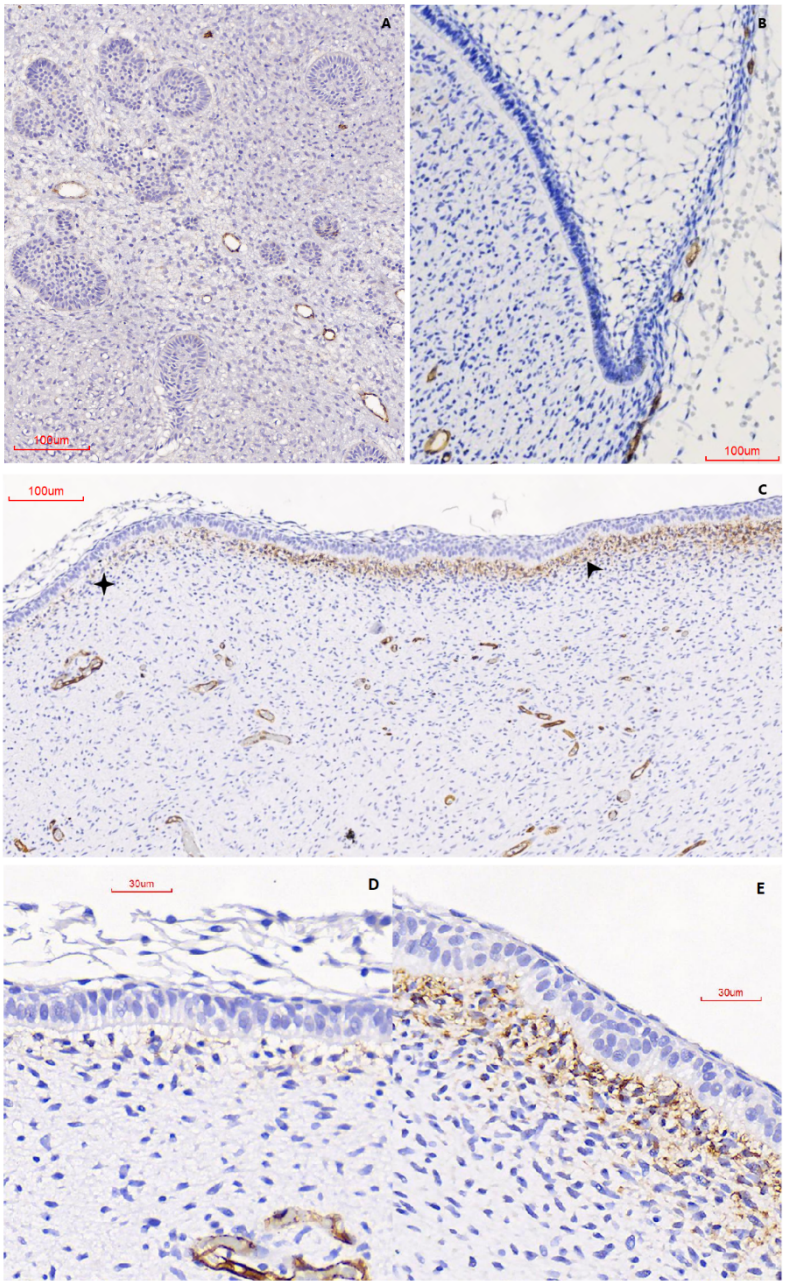

Fig. 2. Immunoexpression of CD34 in (A) AF, (B) TG and (C) POT. Sub-epithelial expression in POT can be observed to vary from a CD34 negative region (black star, left, D) to a negative one (black arrowhead, right, E) which correlates with a decrease in sub-epithelial cell condensation.

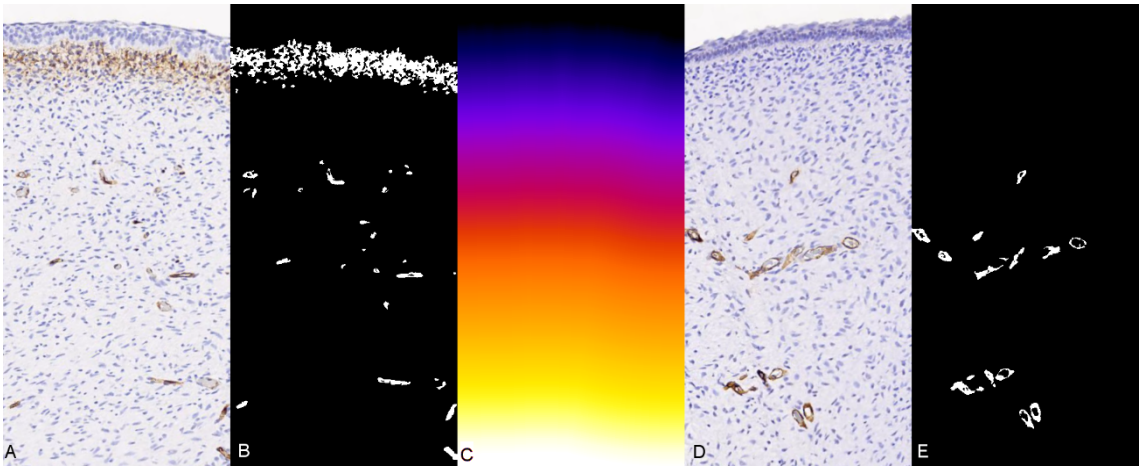

Fig. 3. A) POT immunohistochemical CD34 sub-epithelial positive expression. B) Segmentation of A, showing a binary image. The white regions indicate the presence of CD34 in sub-epithelial mesenchymal cells and blood vessel endothelium. C) The Euclidean distance transform was used to encode the image with values (shown in false colour) corresponding to the distance between each pixel belonging to the tissue in A, and the tissue boundary (given by the empty background). The depth from the boundary of each CD34+ pixel (shown in white in B) can therefore be determined by examining the corresponding pixel values in image C. D) POT immunohistochemical CD34 sub-epithelial negative expression. E) Segmentation of A, showing a binary image. The white colour indicates the presence of CD34 in blood vessels. The process was repeated for other 99 images.

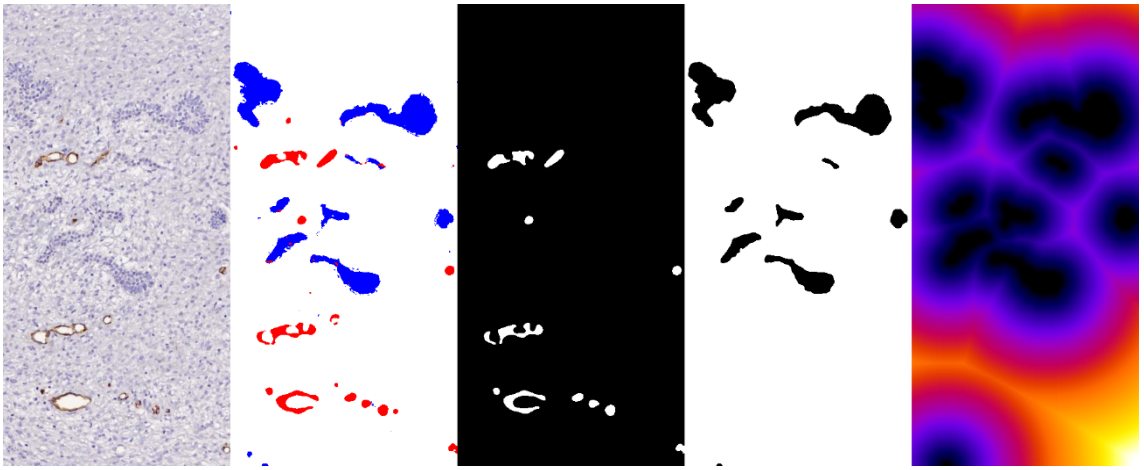

Fig. 4. CD34 expression analysis of AF sections. A) CD34 immunoexpression in AF. B) Segmentation obtained with Labkit, blue: epithelial islands, red: vascular endothelium, white: mesenchyme. C) Binary image of the boundaries of vessel segmentation after image cleaning of small regions. D) Binary image of epithelial islands segmentation. E) The Euclidean distance transform encodes as a pixel value the distance of each white pixel in D to the nearest black region (also in D). The distance of each white feature in C to the black features in D can be determined by examining image E. The process was repeated for other 62 images.

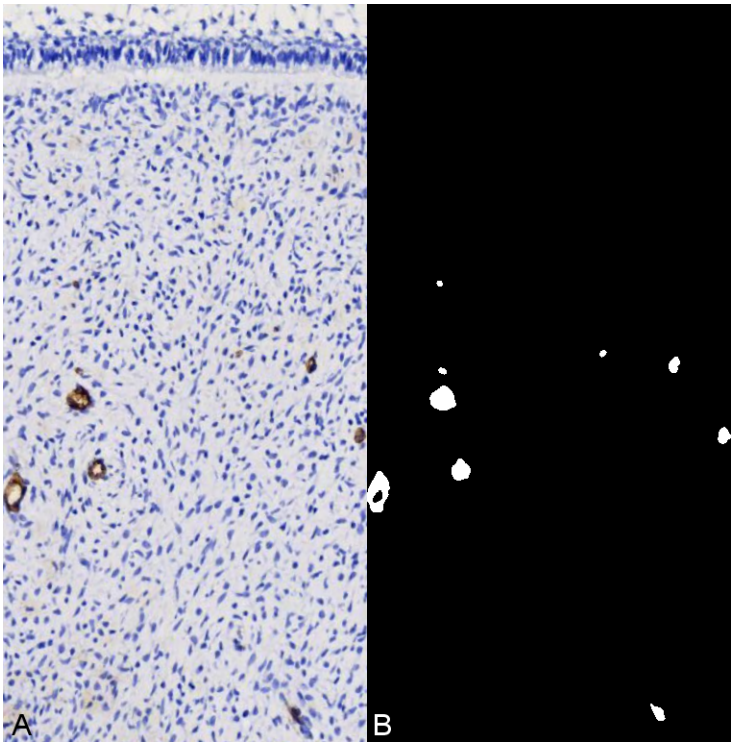

Fig.5. A) TG CD34 expression analysis. B) Segmentation of A, showing a binary image. The process was repeated for other 8 images.

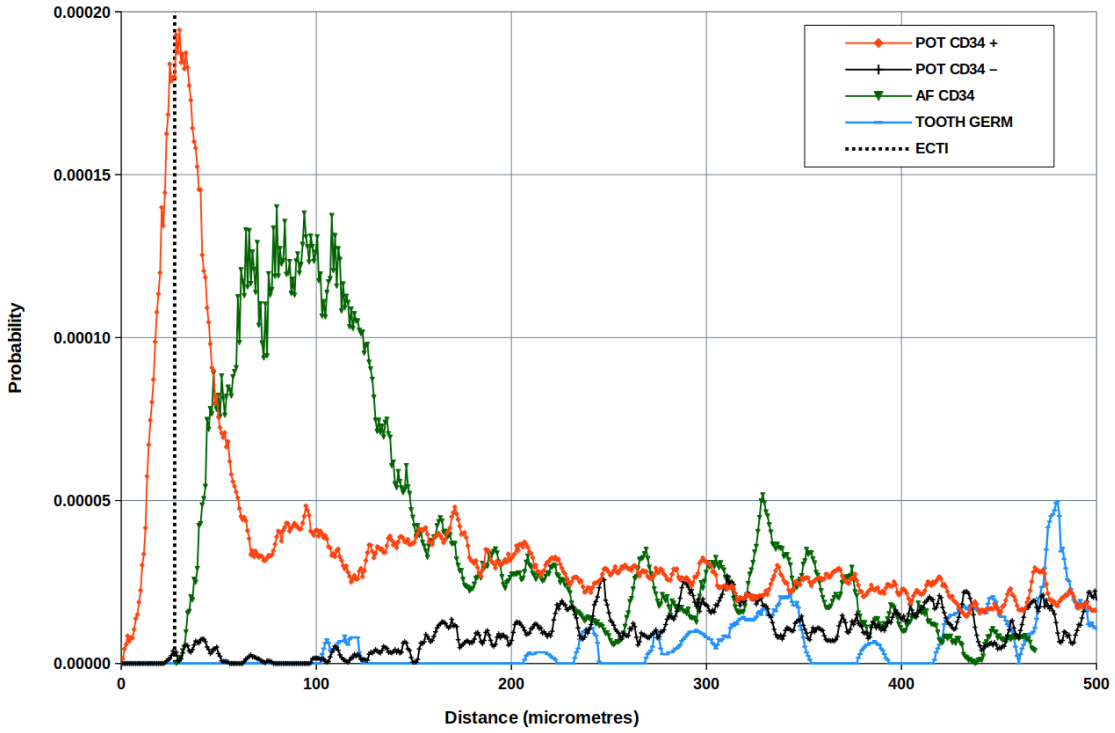

Fig. 6. The graph shows the distribution of distances of CD34 positive pixels to the tissue boundary in all POT images for positive (red) and negative (black) sub-epithelial CD34 expression regions, as well as the distribution of distance from the epithelium between epithelial islands in AF (green) and TG (blue). The AF plot was offset by 27μm, while the TG plot was offset by 6μm to compensate the difference between POT and TG epithelium thickness and the AF plot (which describes the distances from the epithelium rather than from the tissue boundaries). The dotted line indicates the ECTI (epithelial connective tissue interface) in POT samples. Note the differences in distribution between sample types.